Localized, Non-Harmonic Active Flap Motions for Low Frequency In-Plane Rotor Noise Reduction

Ben W. Sim **Mark Potsdam**
US Army AFDD
Ames Research Center
ben.w.sim@us.army.mil *mark.potsdam@us.army.mil*

Cahit Kitaplioglu
Aeromechanics Branch
NASA Ames Research Center
cahit.kitaplioglu@nasa.gov

Philip LeMasurier **Peter Lorber** **Joseph Andrews**
Sikorsky Aircraft Corporation
Stratford, CT
plemasurier@sikorsky.com *plorber@sikorsky.com* *joseph.andrews@sikorsky.com*

ABSTRACT

A first-of-its-kind demonstration of the use of localized, non-harmonic active flap motions, for suppressing low frequency, in-plane rotor noise, is reported in this paper. Operational feasibility is verified via testing of the full-scale AATD/Sikorsky/UTRC active flap demonstration rotor in the NFAC's 40- by 80-Foot anechoic wind tunnel. Effectiveness of using localized, non-harmonic active flap motions are compared to conventional four-per-rev harmonic flap motions, and also active flap motions derived from closed-loop acoustics implementations. All three approaches resulted in approximately the same noise reductions over an in-plane three-by-three microphone array installed forward and near in-plane of the rotor in the near-field. It is also reported that using an active flap in this localized, non-harmonic manner, resulted in no more than 2% rotor performance penalty, but had the tendency to incur higher hub vibration levels.

NOMENCLATURE

A_f	Maximum active flap displacement, deg.
BPF	Blade passing frequency, Hz.
C_T/σ	Thrust coefficient to rotor solidity ratio
M_{AT}	Advancing tip Mach number
M_H	Rotational (Hover) tip Mach number
NM	Noise metric, peak-to-peak value
R	Blade radius
α	Shaft tilt (un-corrected), deg.
μ	Advance ratio
ψ	Azimuth angle, deg.
θ	Elevation angle, deg.
Θ_0	Collective control angle, deg.
Φ_f	Active flap control phase angle, deg.

Presented at the American Helicopter Society 68th Annual Forum, Fort Worth, Texas, May 1-3, 2012.

INTRODUCTION

Exploration of active rotor technologies for aeromechanics benefits on future helicopters is an on-going effort actively pursued by the rotorcraft industry and government laboratories. Many of these active control concepts (Refs. 1-4) were originally conceived for rotor performance improvement, vibration reduction and blade-vortex interaction noise mitigation. All investigations to-date have shown that effectiveness of these active controls lie in their ability to introduce rotating-frame cyclic variations, of two-per-rev or greater, to augment blade motions and blade airloads.

Recent studies (Refs. 5, 6) have identified that low frequency, in-plane rotor noise, primarily of concern to the military, can be attenuated with active controls as well. First proposed in 2008, researchers at the U.S. Army Aeroflightdynamics Directorate (AFDD) and at the University of Maryland, suggested that blade thickness noise (usually dominant near the plane of rotor at moderate-to-high advancing tip Mach numbers), can be suppressed by "anti-noise" pulses generated from specially tailored harmonic active flap motions. Noise reductions were found to be associated with an increase in the in-plane blade loads on the advancing side of the rotor that produced a positive-

peak loading noise pulse. With correct timing/phasing, this "anti-loading noise" pulse had the potential to negate the negative-peak pressures associated with blade thickness noise that predominantly radiates forward and in-plane of the rotor.

This new noise reduction strategy was validated by experimental results obtained from a full-scale Boeing-SMART active flap rotor (Ref. 7) tested in 2008. Up to 6 dB noise reduction was achieved with the use of three and four-per rev harmonic active flap motions. Results indicated that, while the active flap was moving in a harmonic manner around the rotor azimuths, the pertinent "anti-loading noise" pulse, resulting in noise cancellation forward, in-plane of the rotor, originated only from active flap motion near the advancing side of the rotor (around 90˚ azimuth).

It is therefore postulated that, for in-plane noise suppression, the active flap is only required to be deployed locally on the advancing side of the rotor and not on the retreating side - which has no bearing on the acoustics radiation forward of the rotor. Such a localized, non-harmonic active flap motion is perhaps more efficient, non-intrusive and directionality forgiving, given the limited amount of flap actuation authority and conservative blade load limit. This approach also frees up the active flap usage so that it can be deployed at non-advancing side azimuths to meet other aeromechanic objectives. Gopalan and Schmitz (Ref. 6) have reported analyses akin to such non-harmonic actuations and have illustrated the feasibility of using a localized, non-harmonic in-plane force controller to reduce in-plane rotor noise. Similar strategies have been recently proposed by Fogarty et al. (Ref. 8) for blade-vortex interaction noise reductions using active blade twist, and also by Sargent et al. (Ref. 9) for in-plane noise reductions using active blade tip blowing.

This paper will illustrate, for the first time, the feasibility of using such localized, non-harmonic active control strategy for low frequency noise reductions forward and near in-plane of the rotor. Results from an active flap rotor recently tested in an anechoic wind tunnel, will be presented to highlight effects of a AFDD-designed active flap motion that operated only on the advancing side of the rotor. These results will also be compared to measured acoustics radiation from conventional four-per-rev harmonic active flap motions and also from active flap motions derived from closed-loop acoustics investigations.

SIKORSKY ACTIVE FLAP DEMONSTRATION ROTOR TESTING

The opportunity to experiment with localized, non-harmonic active flap motions came about during a joint Sikorsky/UTRC/U.S. Army wind tunnel test program in 2010 (Ref. 10). This was an effort to demonstrate active rotor technologies and their benefits under a Technology Investment Agreement between Sikorsky/UTRC and the U.S. Army Aviation Applied Technology Directorate (AATD). Funded under AATD's High Performance Rotary Wing Vehicle Designs Program, Sikorsky/UTRC modified a full-scale S-434™ rotor with a high authority active trailing edge flap system to explore the feasibility of reducing vibration by at least 20%, acoustic detection by at least 6 dB, and increase maximum blade loading by at least 16%.

Rotor Hardware

The modified active flap demonstration rotor was installed on the Air Force's National Full Scale Aerodynamics Complex's (NFAC) Rotor Test Apparatus (RTA), in the 40- by 80-Foot anechoic test section (Fig. 1), in early October 2010 and was tested for forward flight from January to February 2011 (Refs. 10, 11). A total of 55 hours of blade-on forward flight-testing was conducted with flight envelopes ranging from 40 to 150 knots at various shaft tilt angles and thrust settings.

The rotor itself was derived from a full-scale, 2,900 lb. gross weight, four-bladed S-434™ helicopter. The rotor head, blade cuffs, and swash-plate were production S-434™ components, but with production blades modified to accommodate the active flaps, actuators, wirings, and other required structural supports. Leading edge weights were added to recover dynamic stability. A second cuff was introduced to allow the active flap to pitch the entire blade more efficiently. This resulted in an extension of the blade radius from 165 to 175 inches. Rotor speed was, hence, reduced from 450 to 425 RPM to maintain realistic tip speeds and to stay within centrifugal load limits on the production hub. However, operating rotor speed was limited to 415 RPM during the test to stay below an RTA drive system torsional mode. The second cuff was also locked in forward flight to avoid blade instability (Ref. 13). While test points were acquired between 500 and 3000 lbs thrust, results reported in this paper only focus on a thrust setting of approximately 1550 lbs.

Main Rotor

Rotor Blade	: Sikorsky S-434™
Number of Blades	: 4
Radius	: 175.08 in.
Chord at tip	: 7.99 in.
Chord at flap	: 8.40 in.
Chord inboard	: 6.82

Active Flap

Length	: 20 in.
Chord	: 1.88 in.
Mid-point station	: 126.06 in.
Deflection range	: ±12 deg.

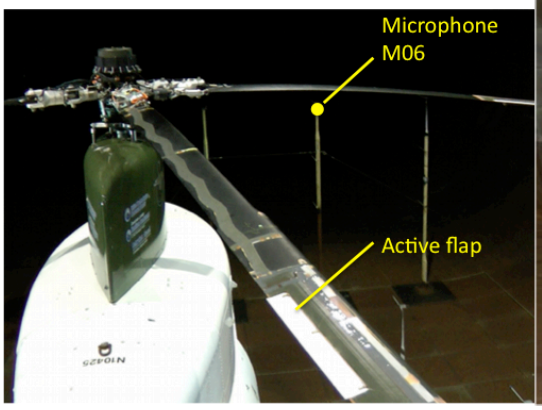

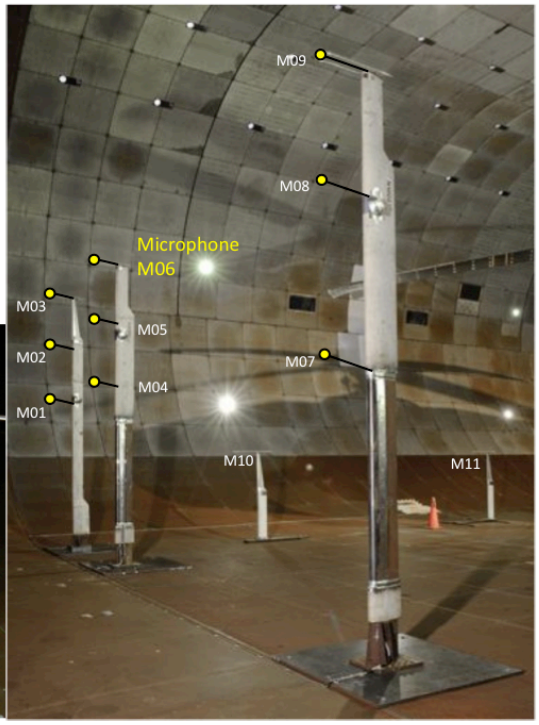

Figure 1. Sikorsky active flap demonstration rotor in NFAC 40- by 80-Foot Wind Tunnel.

Each modified S-434™ production blade contains an embedded electro-mechanical actuator designed to drive an 11.4% span trailing-edge flap (located between 66.3% to 77.7% span station) at frequencies up to five-per-rev. As much as ±9 degrees flap deflection angle, at one-per-rev, was demonstrated from whirl-tower hover testing (Ref. 10). Actuator performance degraded with frequency resulting in flap deflection of about ±1.7 degrees at five-per-rev. Flap rotation stops were geometrically fixed at ±12 degrees. Inputs to the four blades are phased azimuthally such that each active flap received the same command at a given azimuth from a closed-loop (flap position) controller. More details of the blade integration, actuator/flap design, and aerodynamic and aero-elastic analytical results are described in Reference 12.

During the wind tunnel test, the actuators were controlled by a combination of a UTRC open loop controller/health monitor and a high band-width (up to ten-per-rev) Sikorsky Active Rotor Controller (ARC, Ref. 13). The ARC is a linear frequency domain T-matrix controller that is related to the fixed frame Active Vibration Controllers (AVC) implemented by Sikorsky on several current production aircraft. A new fully instrumented rotor shaft and swash-plate control system adapter was also designed by Sikorsky to mate with the RTA. This installation takes advantage of both the RTA primary high authority control system operated by the NFAC model operator, and the RTA dynamic control system, which provides upward of two degrees of authority for the Sikorsky ARC to maintain rotor trim.

Acoustics Instrumentation

A total of eleven microphones were strategically placed around the model to capture rotor noise sources of interest (Fig. 1). Nine of these (M01 to M09) were grouped into a three-by-three rectangular array for low frequency, in-plane rotor noise mapping on the advancing side of the rotor. The microphones were mounted on three separate tower struts, and were positioned near in-plane of the rotor approximately 7 to 20 degrees below wind tunnel horizon. Two other microphones (M10 and M11) were positioned underneath the rotor to capture out-of-plane, blade-vortex interaction noise. All microphones were located within the acoustically-treated portion of the 40- by 80-Foot test section. Note that this geometric/spatial constraint resulted in all microphones to be no more than 2.7*R* away from the rotor – rendering acoustics measurement to be near-field at best. Summaries of the microphone positions, relative to both the rotor hub center and to the advancing blade tip (both at zero shaft tilt), are illustrated in Tables 1 and 2 respectively.

Instrumentation-grade 1/2-inch free-field condenser microphones (G.R.A.S. Type 40AC) with nose cone

fairings were used for the acoustic measurements. Microphone signals were pre-amplified at the source to minimize signal loss over the long wiring runs leading to a junction box housed below the test section - from which the signals were sent to both an acoustic monitoring station and to the data acquisition console. Microphone gains were adjusted at the monitoring station on a per-test point, per-channel basis to maximize signal-to-noise ratio. In addition to the microphone signals, encoders on the rotor shaft provided a one-per-rev trigger signal, as well as a 256-per-rev and a 1024-per-rev sampling clock.

Table 1. Microphone positions[a] (hub-centered).

	Cartesian-coordinates[b]			Spherical-coordinates[c]		
Mic.	***X*,ft**	***Y*,ft**	***Z*,ft**	***r/R***	**ψ,deg**	**θ,deg**
M01	-35.2	18.0	-12.7	2.85	153.0	-17.8
M02	-35.2	18.0	-8.5	2.77	152.9	-12.1
M03	**-35.2**	**18.0**	**-4.6**	**2.73**	**152.9**	**-6.7**
M04	-34.6	9.8	-12.2	2.60	164.3	-18.7
M05	-34.2	9.8	-8.7	2.51	164.1	-13.8
M06	**-35.4**	**9.8**	**-4.6**	**2.54**	**164.5**	**-7.2**
M07	-34.9	2.4	-12.2	2.54	176.1	-19.2
M08	-34.9	2.4	-8.8	2.48	176.1	-14.0
M09	**-34.9**	**2.3**	**-4.7**	**2.42**	**176.3**	**-7.6**
M10	-19.9	11.9	-13.9	1.85	149.2	-30.9
M11	-8.8	14.1	-13.9	1.48	121.9	-39.9

[a] Zero shaft tilt. *X-Y* plane parallel to ground.
[b] Positive *X* points aft. Positive *Y* towards advancing side. Positive *Z* points up.
[c] Azimuth ψ rotates counter-clockwise. ψ = 0° aft. Elevation θ is positive above horizon. θ = 0° parallel to horizon.

Table 2. Microphone positions[a] (advancing blade tip-centered).

	Cartesian-coordinates[b]			Spherical-coordinates[c]		
Mic.	***X*,ft**	***Y*,ft**	***Z*,ft**	***r/R***	**ψ,deg**	**θ,deg**
M01	-35.2	3.4	-12.7	2.58	174.5	-19.8
M02	-35.2	3.4	-8.5	2.49	174.5	-13.5
M03	**-35.2**	**3.4**	**-4.6**	**2.44**	**174.4**	**-7.4**
M04	-34.6	-4.8	-12.2	2.54	188.0	-19.2
M05	-34.2	-4.8	-8.7	2.44	188.0	-14.2
M06	**-35.4**	**-4.8**	**-4.6**	**2.47**	**187.7**	**-7.4**
M07	-34.9	-12.2	-12.2	2.67	199.2	-18.2
M08	-34.9	-12.2	-8.8	2.61	199.3	-13.3
M09	**-34.9**	**-12.3**	**-4.7**	**2.56**	**199.4**	**-7.2**
M10	-19.9	-2.7	-13.9	1.67	187.8	-34.7
M11	-8.8	-0.5	-13.9	1.13	183.3	-57.6

[a] Zero shaft tilt. *X-Y* plane parallel to ground.
[b] Positive *X* points aft. Positive *Y* towards advancing side. Positive *Z* points up.
[c] Azimuth ψ rotates counter-clockwise. ψ = 0° aft. Elevation θ is positive above horizon. θ = 0° parallel to horizon.

Data Acquisition

Data acquisition and model rotor control feedbacks were accomplished using a coupled set of Sikorsky/ UTRC and NFAC systems that were synchronized to within a few rotor revolutions from each other.

The Sikorsky/UTRC system was primarily responsible for acquisition of data streams from the active flap sensors, the rotor head and blade instrumentation, and the RTA accelerometers. This system consisted of two National Instruments PXI/ LabView data acquisition units configured to signal condition and acquire up to 128 channels of "high speed" data. These data were acquired at a fixed sampling rate of 2 kHz and subsequently interpolated in post-processing to 256 points–per-revolution. An additional 64 channels of "steady-state" data was also used for Safety-of-Flight (SOF) monitoring.

The NFAC system comprised of two sub-units. First is the lower bandwidth BDAS primarily responsible for logging wind tunnel conditions, RTA drive system state, rotor balance data and primary /dynamic swash-plate controls. The second sub-unit consist of the higher bandwidth DDAS for pressure transducers and acoustic measurement. All channels, except those corresponding to surface pressure and acoustic measurement, were post-processed to 256 samples-per-revolution using the sampling clock from the rotor encoder. Surface pressure and acoustics data were separately acquired at a higher rate of 1024 samples-per-revolution to capture higher frequencies.

Acquired channels are post-processed via azimuth-based averaging of multiple revolutions of steady-state, periodic data. In most cases, at least 9.25 seconds of data were acquired - which amounts to having more than 64 rotor revolutions of data available for azimuth-based averaging. This procedure isolates harmonic contents pertaining only to the rotation rate of the rotor, and suppresses all other unwanted frequency content, to achieve superior signal-to-noise ratio.

Test Conditions

While the scope of the wind tunnel test embodied a wide variety of flight conditions, this paper only focus on the 120 knots level flight case - corresponding to an advance ratio of 0.32. At this nominal condition, the shaft tilt (un-corrected) was –5.0 degrees, and the rotor operated at an advancing tip Mach number of 0.753 with a thrust-to-solidity ratio of 0.046 (approximately 1,550 lb of thrust). For all the test points investigated in this paper, the rotor was trimmed to the same thrust, with minimum hub moments (pitch and roll), using Sikorsky/UTRC's Active Rotor Controller.

ACOUSTICS DATA QUALITY

Non-ideal anechoic wall treatment in the 40- by 80-Foot test section creates opportunities for acoustic pressure waves to be reflected (Ref. 14), particularly at frequencies below 100 Hz. This introduces uncertainties in noise measurement for the first three blade-passing harmonics, at 27.7, 55.3 and 83.0 Hz, for the active flap demonstration rotor operating at a nominal rotor speed of 415 RPM. Distortions in the acoustics time histories can be prevalent when spurious acoustics waves, not absorbed by wall treatments at these frequencies, are reflected into the measurement space. In addition, excitation of standing wave patterns in the enclosure may further distort noise measurements if the modal frequencies coincide with the low frequency rotor tones of interest. Together, these two facility-related issues can render low frequency rotor noise measurement to be highly problematic. Acquired data, therefore, must be carefully scrutinized to ensure that true rotor noise field and its characteristics are represented.

Ambient/Background Noise

One factor is the ambient noise level present during "wind-on" conditions. Typically, ambient noise is dictated by the facility's fan drive system, but can include distortions from standing wave patterns, motor system sounds and flow-induced sounds from RTA, wall surfaces or acoustics apparatus, such as the tower strut and/or microphone body. For this test, the wind tunnel's variable-pitch fan-drive system was set at the lowest possible fan speed of 98.5 RPM to minimize background noise and to simultaneously avoid having fan drive tones[1] overlapping rotor tones.

Figure 2 illustrates the revolution-based averaged acoustic time history and frequency spectrum for the 120 knots baseline condition[2] (without active flap motions) at the three most in-plane microphones (M03, M06 and M09). Black lines indicate the acoustic pressures from the rotor, whereas green lines indicate the ambient noise obtained from rotating bare hub runs[3]. Good signal-to-noise ratios of at least 12 dB generally exist up to the sixth *BPF*. However, results also indicated that microphones M06 and M03 contained undesirably high ambient noise at the first *BPF*. This effect is particular strong at microphone M06 and can be observed in the acoustics time history with large blade-to-blade differences. While it remains unconfirmed, this is likely an effect associated with standing wave modes across the tunnel cross-section in the lateral direction[4]. This standing wave modal frequency unfortunately coincided with the rotor's first *BPF* at 27.7 Hz. It is quite possible that microphone M06 was positioned near an anti-node that introduced significant noise oscillations; while the almost centerline microphone M09 was near to a node point that saw less of this standing wave effect.

Due to the above-mentioned contamination at first rotor *BPF*, acoustics results in this paper will only consider contents from the second blade-passing harmonic and above. Figure 3 illustrates the results of applying this high-pass filtering to acoustics time histories measured at microphone M03, M06 and M09. General features of the acoustics waveform are preserved with this post-processing technique, while large blade-to-blade differences are suppressed.

Repeatability

Good noise measurement repeatability is also achieved with high-pass filtering of the acoustics data. Figure 4 shows the noise measurement of 14 separate test points corresponding to the 120 knots baseline condition, obtained on different occasions over the duration of the wind tunnel test. Primary features of the acoustic time histories of all 14 test points (black lines) were found to repeat fairly well. Compared to the mean (magenta line), scattering errors of both peak amplitudes and phase appear to be quite small.

Acoustic Reflections

While the high-pass filtering technique was effective in removing some facility effects due to standing waves, strong acoustic reflections associated with frequencies greater than the first *BPF* were also present in the acquired acoustic time histories. As reported in Reference 14, these reflections are primarily due to non-ideal anechoic wall treatment in the 40- by 80-Foot test section. Net results are manifestations of spurious reflections in the measured acoustics time history, as depicted by additional pulses in Figure 5. Note that a reflection-free acoustic time history should only contain four major direct pulses due to each of the four blades. It is also conceivable that some reflections could have been embedded within the direct pulse.

[1] For all six synchronized fan drives, the tones of each of the fifteen-bladed fan occur at multiple integers of 24.6 Hz.

[2] NFAC Run 75, Point 18. Sikorsky Run 108, Point 16.

[3] NFAC Run 70, Point 24. Sikorsky Run 103, Point 22.

[4] Simple standing wave calculations (based on flat, rigid walls) suggest that the wind tunnel's 80-foot lateral span may spawn modal frequencies at multiple integers of 13.8 Hz. It is, therefore, possible that the second mode at 27.6 Hz, was excited by the rotor's first *BPF* at 27.7 Hz.

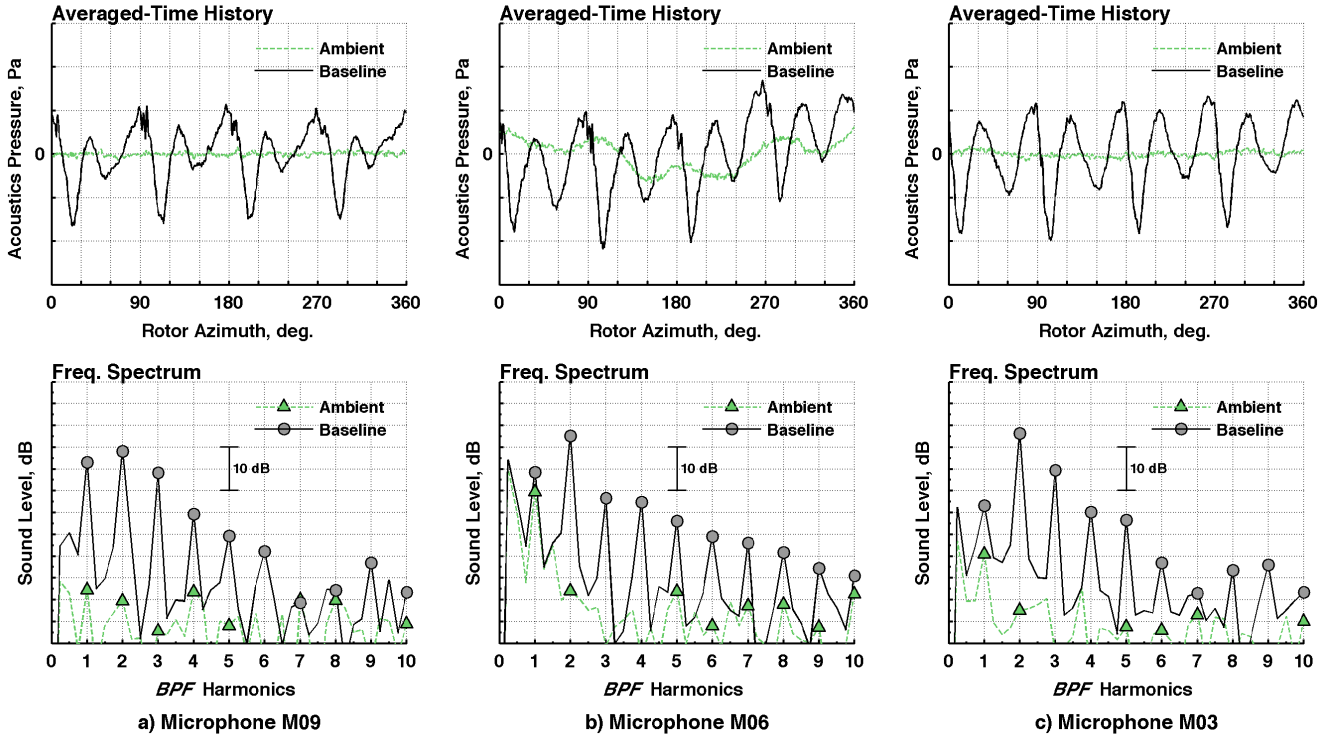

Figure 2. Signal-to-background noise ratios.

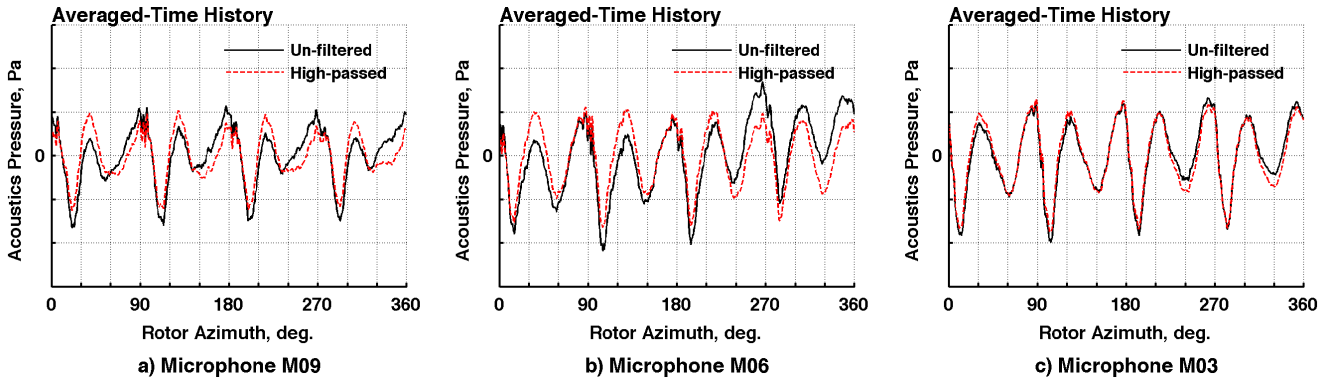

Figure 3. High-pass filtering of measured acoustic time histories.

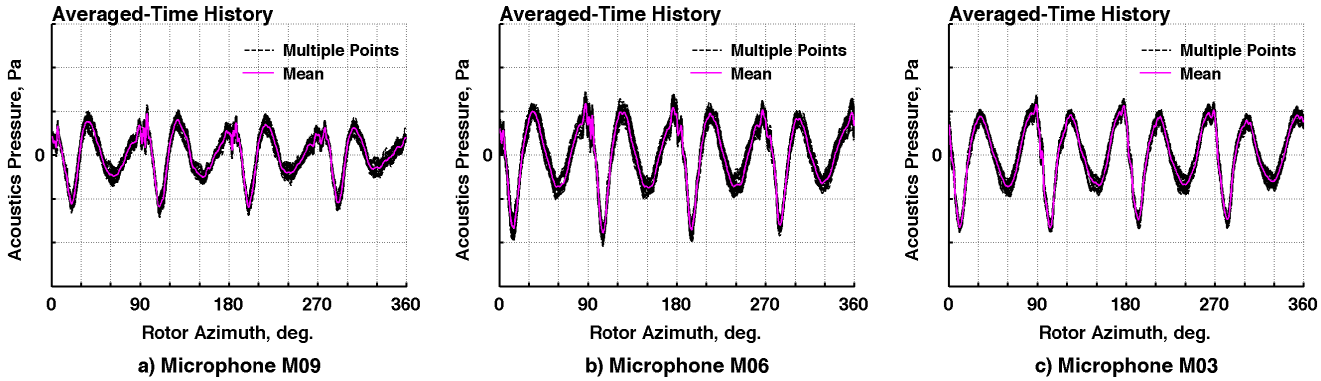

Figure 4. Repeatability of acoustics measurements for baseline condition.

NOISE METRIC

To better isolate the effects of active flap motions on direct rotor noise, additional post-processing and a somewhat rudimentary noise metric was developed to focus only on the direct pulse as best as possible, while minimizing the effects of reflections that obscure true rotor noise radiation characteristics.

An example of the processed acoustic time history is illustrated by the red line shown in Figure 5. Essentially, this red line is an average of the four pulses generated by each of the four blades. The peak-to-peak value, associated with only the direct pulse, is subsequently extracted and used as the noise metric (*NM*) representative of the acoustics state at each microphone and for each test point. Note that this noise metric is qualitative at best because of its inability to disregard reflections that may have overlapped the direct pulse.

For the purpose of comparing changes in the acoustics radiation between test points (usually between the baseline and an active flap case), the proposed noise metric can be expressed in term of a decibel (dB) change as shown by Eq. 1. This expression assumes that reflections embedded within the direct pulse, for the two test points, are of the same fractional amount (k) relative to the direct pulse itself. Even though the noise metric, *NM*, is distorted by embedded reflections, the net change in dB may be representative of the change in the acoustics state between the two test points.

$$\Delta dB = 20 \cdot \log\left(\frac{NM_1 + k \cdot NM_1}{NM_0 + k \cdot NM_0}\right) = 20 \cdot \log\left(\frac{NM_1}{NM_0}\right) \qquad (1)$$

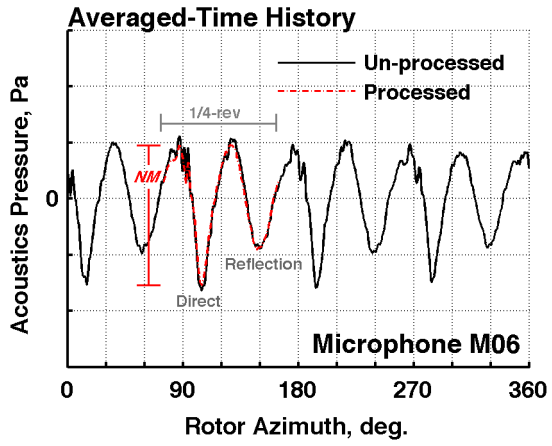

Figure 5. Definition of noise metric, *NM*.

LOCALIZED, NON-HARMONIC ACTIVE FLAP MOTION

This section of the paper reports on effects of using active flap motion in a localized, non-harmonic manner to achieve low frequency, in-plane rotor noise reductions. Figure 6 illustrates an example of such a flap motion developed in-house by US Army AFDD (designated as Model01) with the following properties:

- An increase in the flap angle (positive, flap down) to a maximum displacement of $+A_f$ over a spread of 30˚ azimuth.
- Followed by a region of decreasing flap angle to a minimum displacement of $-A_f$ over 60˚ azimuth.
- Subsequently ends with another increase in flap angle to return to 0˚ over a 30˚ azimuth spread.

Key parameters are the maximum flap displacement amplitude, A_f, and the control phase angle, Φ_f, that defines the azimuth where the decreasing flap angle crosses 0˚. AFDD studies based on extensive CSD/CFD-simulations of a prior active flap rotor test (Ref. 7) have shown that the control phase angle must be in the vicinity of 90˚ azimuth for effective forward, in-plane rotor noise reductions. It was also found that the decreasing flap angle segment is essential to the enabling of forward, in-plane rotor noise cancellations.

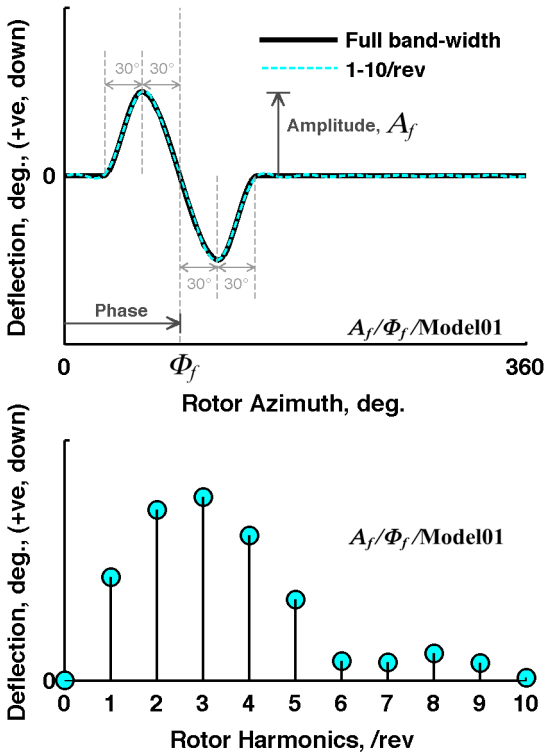

Figure 6. AFDD Model01 waveform.

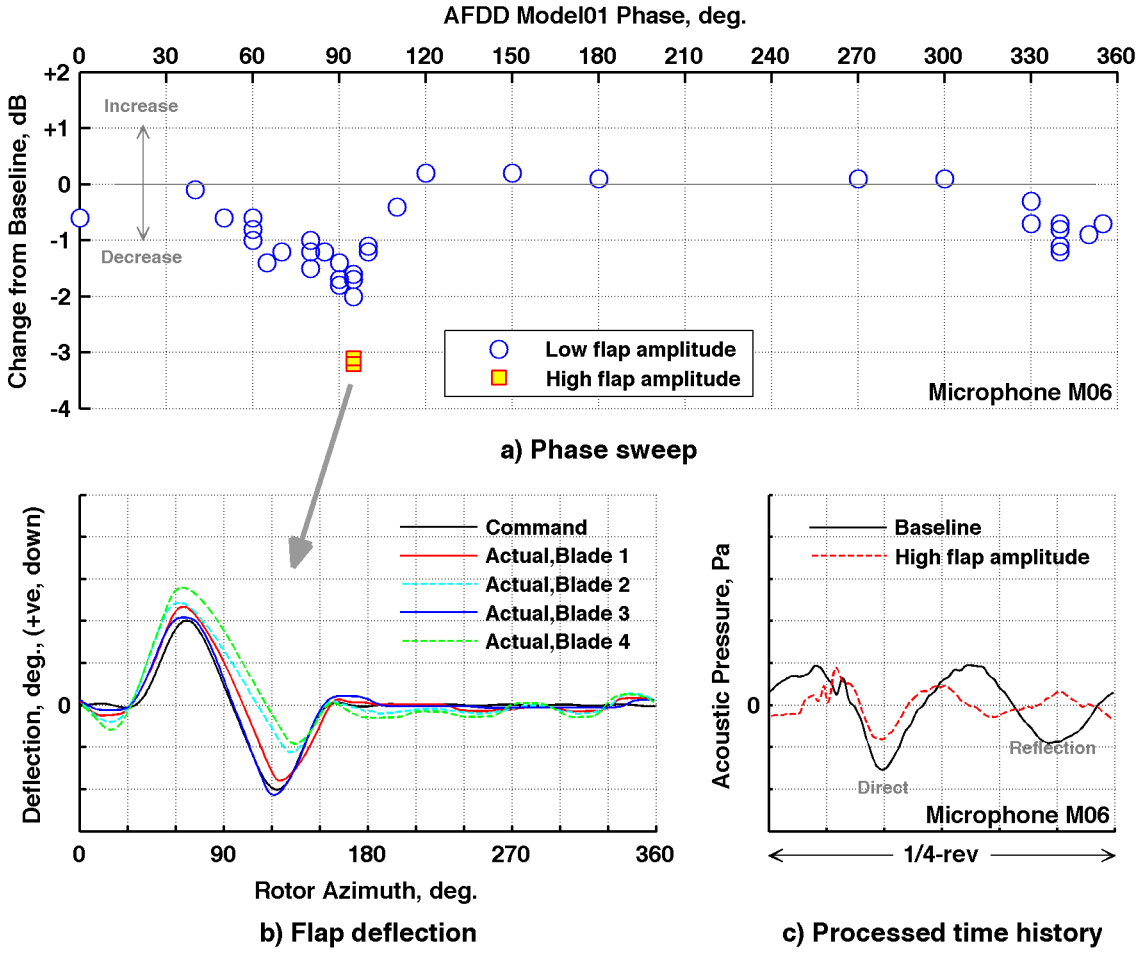

Figure 7. Effects of AFDD Model01 waveform at microphone M06.

Implementation of the Model01 flap motion waveform with Sikorsky/UTRC's bandwidth-limited[5] ARC, is shown by the cyan line in the flap deflection time history (Fig. 6). In general, the required azimuth-varying shape is well represented by the first ten-per-rev rotor frequencies. Spectral composition further shows that most of the actuation demand is in the first five rotational harmonics - with no requirements at zero-per-rev (no constant flap offset) and very little contributions from six-per-rev and beyond.

Results for the Model01 flap motion waveform at different maximum flap displacement amplitude, A_f, and control phase angle, Φ_f, are illustrated in Figure 7a. The net dB change at microphone M06 from baseline (without active flap motion) is plotted as a function of (commanded) control phase angle for a low flap amplitude setting and a high flap amplitude setting[6]. The Model01 flap motion waveform appears to be most effective at a control phase angle of 95˚ with peak-to-peak noise reduced by up to 3.2 dB using the high flap amplitude setting. Note that these test results also indicated a fluctuation of up to ±0.4 dB for some of the repeated test points. For reasons yet unknown, reduced noise levels are also present at control phase angles near 340˚. Operating the Model01 flap motion waveform at these Φ_f values should, in principle, have no bearing on the forward microphone M06.

Another area of concern is the consistency of the active flap motions on all four blades. Figure 7b shows that not all active flaps were deflecting the same, nor in a manner as required by the Model01 flap motion waveform (high flap amplitude setting shown). In general, while it was found that blade 3 conformed best to the prescribed motion, blade 1 typically had a small phase lag of approximately 5˚. Blades 2 and 4 tend to have larger phase lags and also exhibited the inability to extend to more negative flap displacements at higher frequencies, most likely a result of issues in the analog feedback circuits for those two actuators. These excursions from ideal flap motion, and also significant

[5] Sikorsky/UTRC's ARC system tracks up to ten-per-rev.
[6] Approximately twice as large compared to the low flap amplitude setting.

variations between blades, create "smearing" issues that can render the cancellation of in-plane noise using carefully timed "anti-loading noise" pulses to be less effective.

Figure 7c illustrates the processed acoustic time history for microphone M06 that achieved best noise reduction of 3.2 dB at a (commanded) control phase angle of 95˚ with high flap amplitude (NFAC Run 75, Point 76. Sikorsky Run 108, Point 74). Peak-to-peak noise level associated with the direct pulse is reduced - suggesting that a properly timed "anti-loading noise" signal was produced to partially reduce the negative peak. Some high frequency contents were also introduced prior to the direct pulse. These may be residuals from partial cancellations between the "anti-loading noise" and thickness noise. Reflections were also somewhat reduced compared to baseline.

Noise reduction benefits of the afore-mentioned best Model01 flap motion waveform are also prevalent at other microphone locations (Fig. 8). Processed acoustic time histories indicate that noise reductions of the direct pulse are achieved at the three-by-three in-plane microphone array (M01 to M09). Figure 8 also shows that noise reductions become smaller at microphones that are more out-of-plane; and that it is most effective for microphones M07, M08 and M09 residing near the centerline of the wind tunnel. The latter may be explained by the phase lags in the measured active flap motions on blades 1, 3 and 4 (Fig. 7b) that are known to have greater influences on microphones near the centerline strut, and less so on the more advancing side microphones.

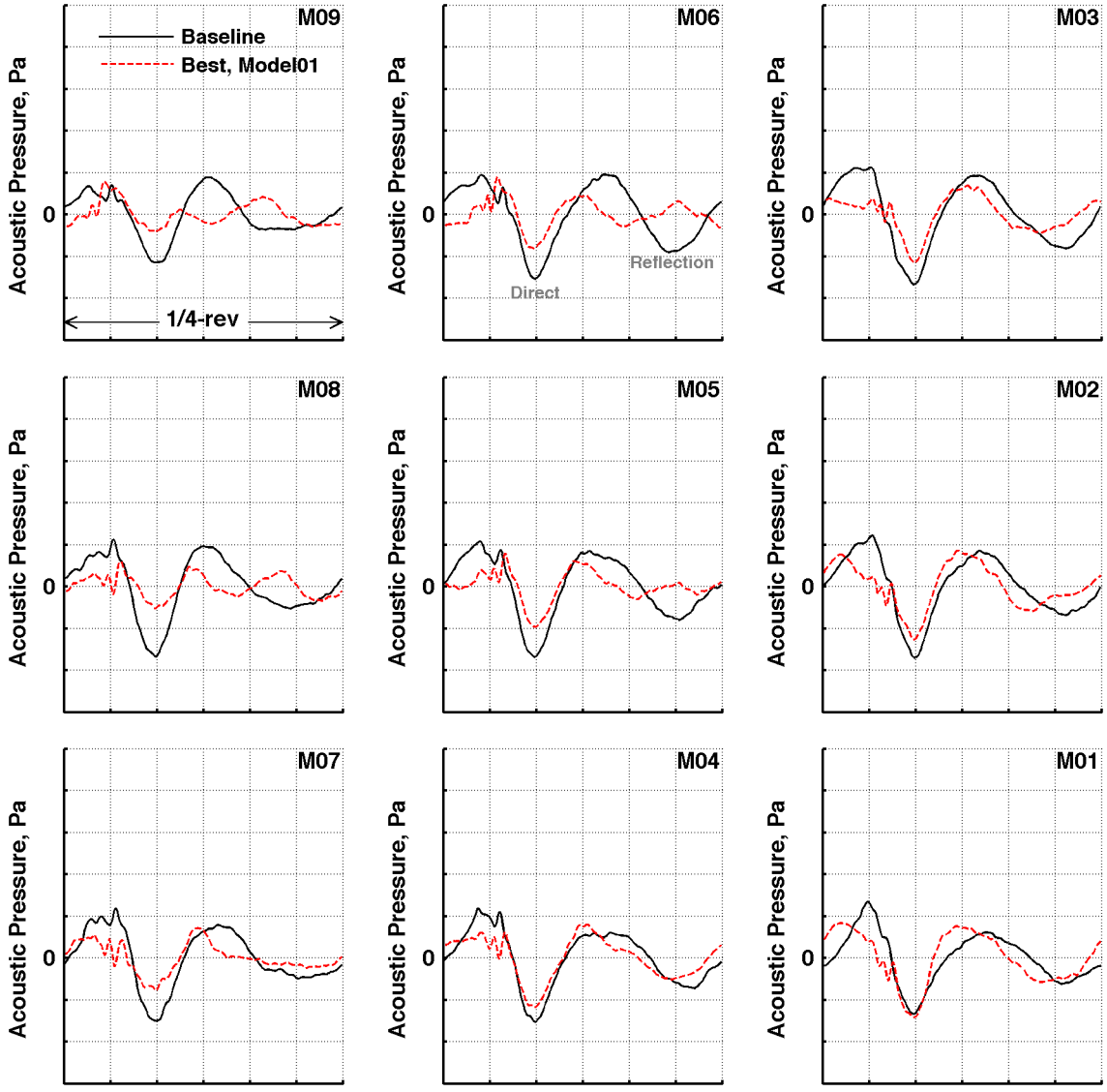

Figure 8. Noise directivity of "best" AFDD Model01 waveform on in-plane microphone array.

FOUR-PER-REV HARMONIC ACTIVE FLAP MOTION

Results for a conventional four-per-rev harmonic actuation of the active flap are illustrated in this section for comparison purposes. In this mode of actuation, active flap motions are no longer restricted to a local portion of the rotor disk, but are (ideally) incurring flap displacements in a sinusoidal fashion at all azimuths.

Figure 9a illustrates the effect of this four-per-rev active flap motion at microphone M06 for different maximum flap displacement amplitudes and phase angles. The largest in-plane noise reduction occurs near 270˚ phase angle, with a 2.7 dB reduction from baseline at the high flap amplitude setting.

Figure 9b shows the measured flap displacements of each blade for this "best" four-per-rev case (NFAC Run 51, Point 35. Sikorsky Run 85, Point 36). Similar to afore-mentioned Model01 runs, the active flap motion of each blade is inundated with blade-to-blade dissimilarities. Worst appears to be blade 4 that operated in a more saw-tooth-liked fashion, rather than the desired sinusoidal waveform. More importantly, the "zero-crossing" of the decreasing active flap displacements near 90˚ azimuth (known to be important for in-plane noise reduction) is phase-lagged by as much as 15˚ when compared to other blades. It is likely that there are "azimuth alignment" issues between the "anti-noise" pulse and the direct thickness pulse from blade 4 - rendering their cancellations to be less efficient. The net processed acoustic time histories at microphone M06 is shown in Figure 9c.

Noise reductions of the direct pulse are achieved across the microphone array as shown in Figure 10. Highest noise reduction levels occur near centerline microphones. Also shown in Figure 10 is that the four-per-rev flap motion resulted in more noise reductions on the advancing side (M01 to M03) than the AFDD Model01 flap motion. This is may be due to "zero-crossings" that occur earlier, before 90˚ azimuth (Fig. 9b), for blades 1 and 3.

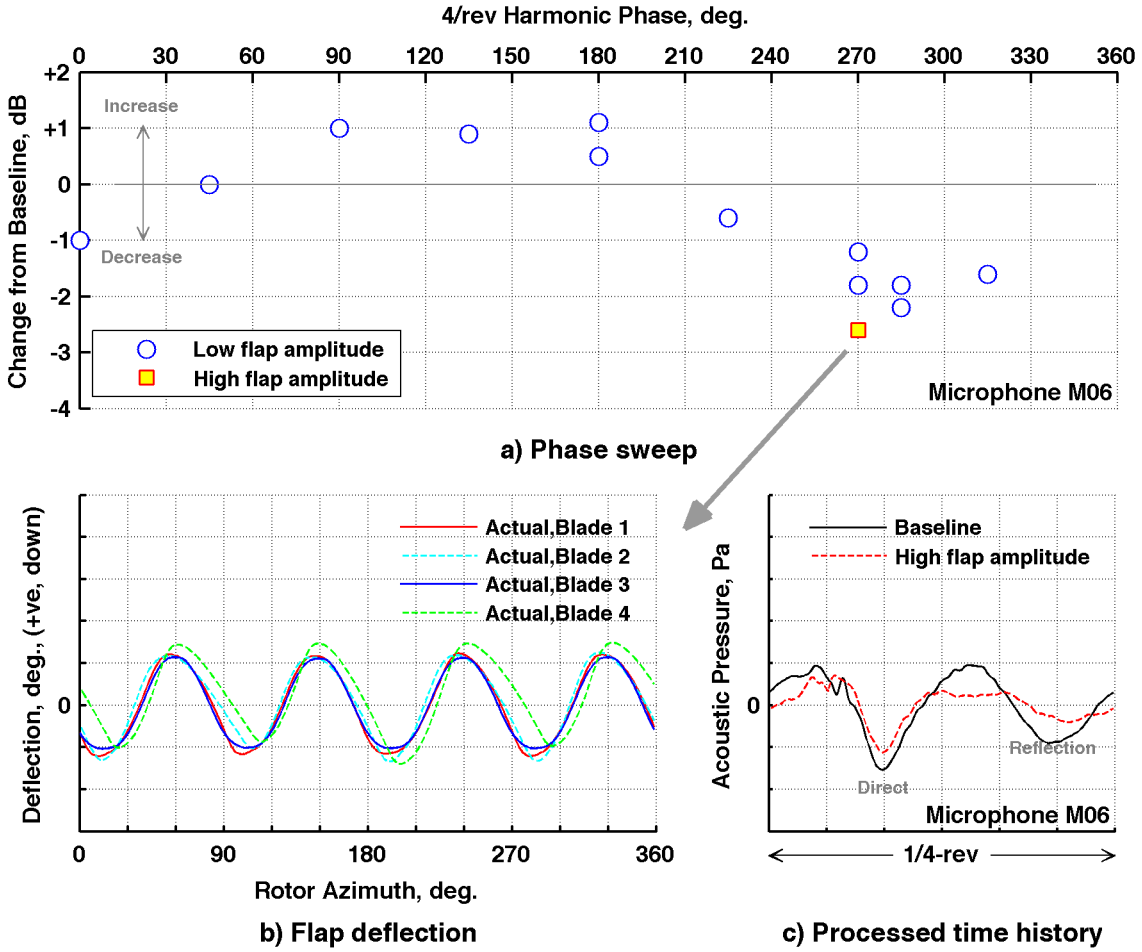

Figure 9. Effects of "best" four-per-rev flap motion at microphone M06.

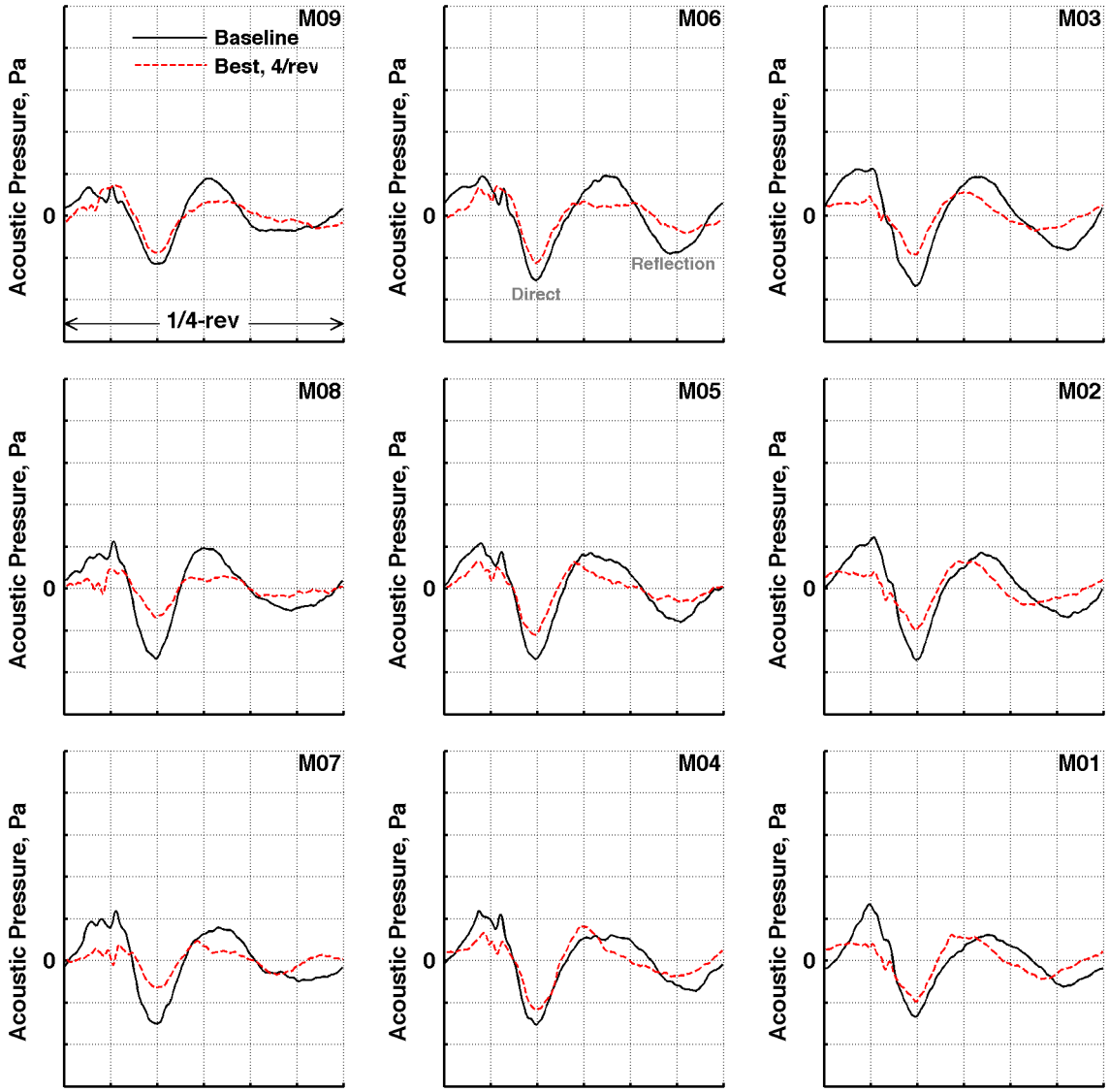

Figure 10. Noise directivity of "best" four-per-rev flap motion on in-plane microphone array.

CLOSED-LOOP ACOUSTICS ACTIVE FLAP MOTION

Closed-loop acoustics measurements were also attempted during the test to derive "optimized" active flap motions for reduced low frequency, in-plane noise levels. Measured acoustics data from microphones M03, M06 and M09 were fed into the Active Rotor Controller (ARC) to enable active flap motion solutions, associated with the lowest programmed "cost", to be identified in near real-time. This section will present results from one such case (NFAC Run 75, Point 84. Sikorsky Run 108, Point 83) where the "cost" function of the optimization routine is defined by the low frequency harmonic noise contents, equally weighted, at the three in-plane microphones.

The active flap motion generated by ARC is shown in Figure 11a. Maximum flap amplitude is somewhere between those specified for the non-harmonic Model01 active flap motion and for the four-per-rev harmonic active flap motion. For reasons unknown yet, the active flap was commanded to move, not only on the advancing side, but also on the retreating side as well (between 300˚ to 360˚ rotor azimuth). Corresponding noise measurements at microphone M06 are illustrated in Figure 11b. Measurements show small reductions of the direct pulse from baseline, but considerable reductions in the ensuing reflections. Noise reduction levels on the in-plane microphone array (Fig. 12) are generally on par with those for the non-harmonic Model01 and four-per-rev harmonic active flap motion.

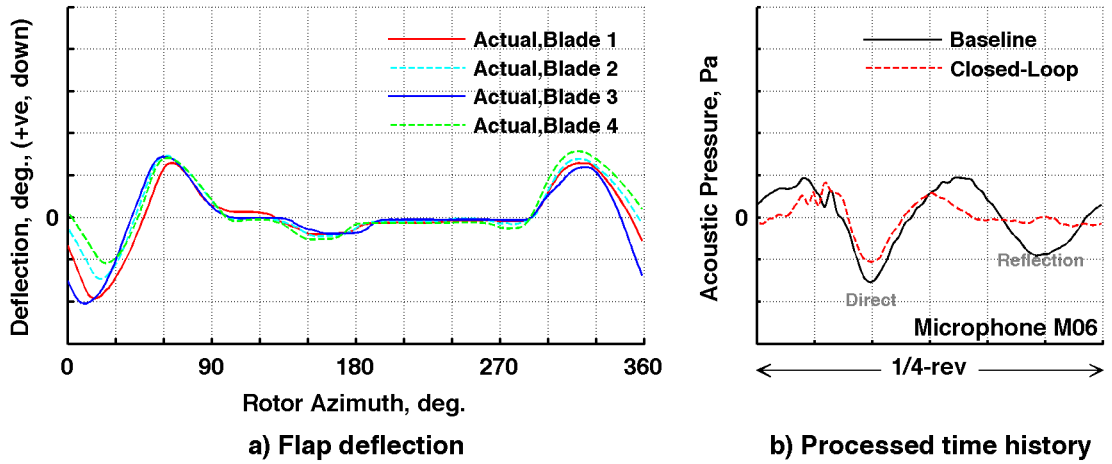

a) Flap deflection b) Processed time history

Figure 11. Effects of closed-loop acoustics active flap motion at microphone M06.

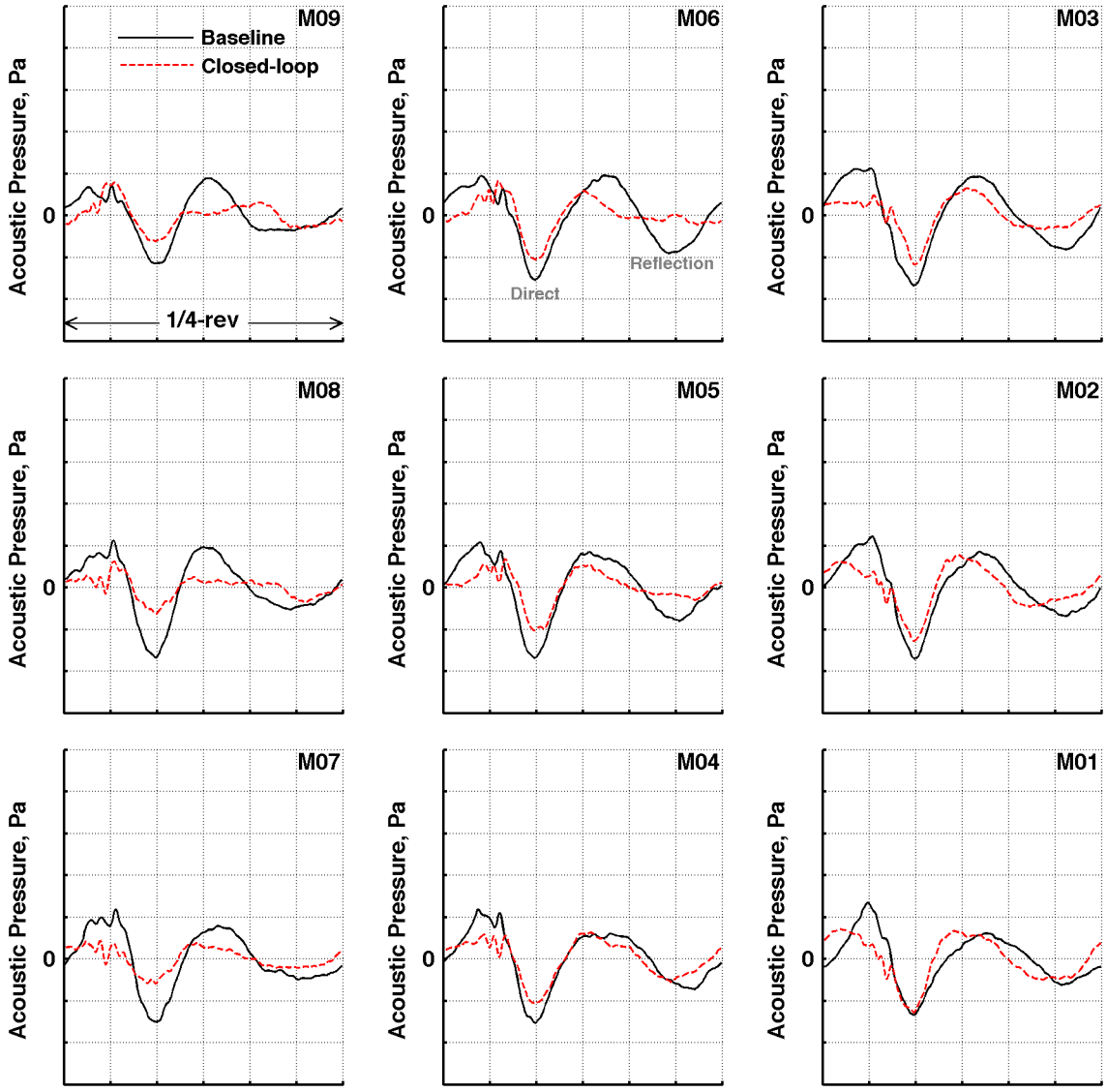

Figure 12. Noise directivity of closed-loop acoustics active flap motion on in-plane microphone array.

DISCUSSION & IMPLICATIONS

A comparison of the measured active flap motions (blade 1) for the three different actuation schemes is illustrated in Figure 13. All three schemes resulted in approximately the same amount of noise reductions at the in-plane microphone array (Figs 8, 10 and 12). Of interest to note is the similarity of these 'best" active flap motions on the advancing side of the rotor, between 30˚ to 100˚ rotor azimuth. This feature is key for enabling forward, in-plane noise reductions.

Similar trends have been observed in a separate active flap rotor test reported in Ref. 7. It was reported that noise reductions were attributed to "anti-loading noise" pulses resulting from the use of active flap motions to increase in-plane force on the advancing side of the rotor (Refs 5 and 7). This was achieved primarily through dynamic changes in the blade torsion (twisting) that caused local changes in the angle-of-attack, and hence, the local blade aerodynamics. The governing criterion is to generate an increase in the in-plane force as the blade rotates through the advancing side (mostly between 60˚ to 120˚ rotor azimuths).

The same behavior is observed in this test. For all active flap motions that led to noise reductions (Fig. 13), a similar (dynamic) torsion trend was found on the advancing side of the rotor, between 60˚ to 120˚ rotor azimuths (Fig. 14a). These results are based on measurements obtained at 0.61*R* (near the flap), and are plotted relative to the baseline condition to illustrate augmented blade torsions due to active flap motions. Note that AFDD Model01 waveform introduced some residual torsion on the retreating side - resulting in a four-per-rev-liked excitation possibly caused by operating near the first blade torsion mode[7].

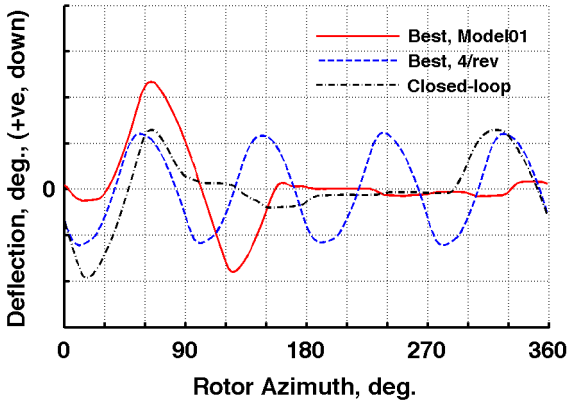

Figure 13. Comparisons of "best" active flap motion schemes (blade 1).

Similar plots are shown for flap-wise bending moments (Fig. 14b) and chord-wise bending moments (Fig. 14c). A general increase in the flap-wise bending moment (relative to baseline) is observed near 90˚ rotor azimuth. No distinct correlations are observed for chord-wise bending moments, with the exception of the four-per-rev flap motion resulting in much stronger response compared to others.

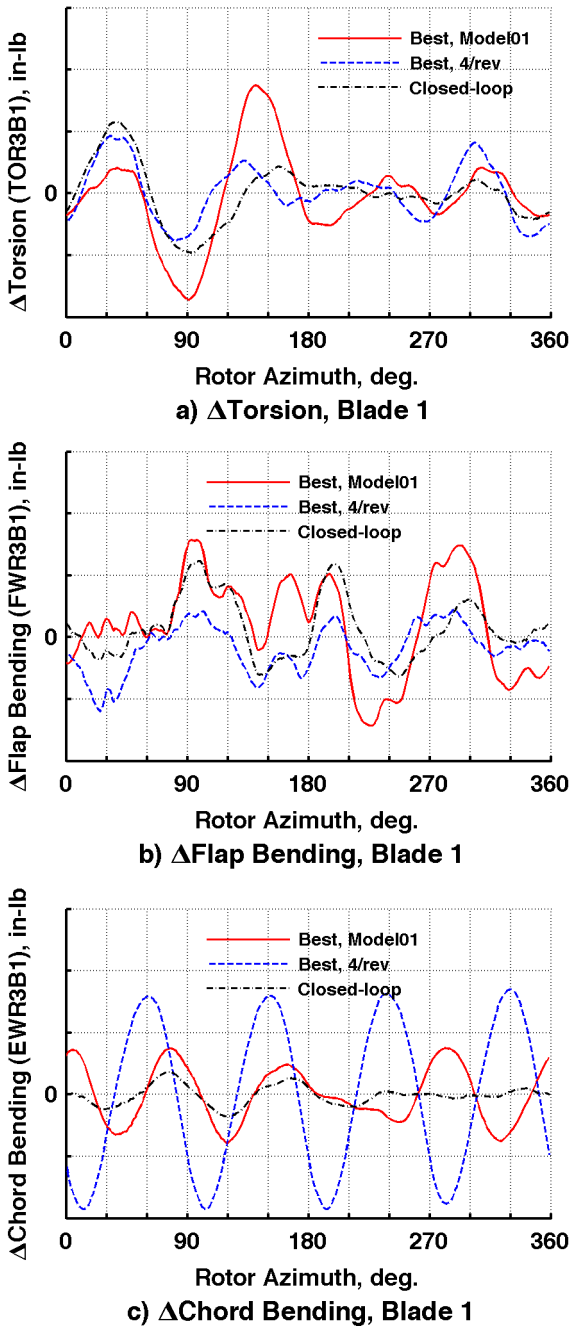

Figure 14. Comparisons of strain gage measurements (blade 1, 0.61*R*) for the "best" active flap motion schemes.

[7] Reference 10 reported a predicted first torsion mode of near five-per-rev for this rotor with locked secondary cuff.

Measurements indicative of the rotor trim state are illustrated in Figure 15a via changes in the rotor thrust, pitch moment and roll moment, relative to their baseline counterparts. The rotor was well trimmed for all "best" active flap cases, as evident by no more than 50 lb variations in measured rotor thrusts (relative to baseline). Hub moments, in general, were also well trimmed – with pitch and roll moments deviating from baseline values by less than 50 in-lb. Although the difference in roll moments between the AFDD Model01 waveform and the four-pre-rev flap motion was as much 90 in-lb, such small deviations are generally deemed acceptable for full-scale rotor operations.

Figure 15b illustrates changes in rotor performance via percentage changes of measured rotor thrust, torque and the overall lift-to- equivalent drag ratio, relative to baseline. While rotor thrusts remained in trim to within 3% of the baseline, the active flap cases universally resulted in increased rotor torques of approximately 1.9% to 2.3 %. Note that the high rotor torque associated with AFDD Model01 waveform may be due to the presence of strong four-per-rev variations in the measured blade torsions; which nearly had the same order of magnitude as the blade torsions measured for the four per- rev flap (Fig. 14a). As a result, lift-to-drag ratios (*L/D*), an indicator of the rotor's aerodynamic efficiency, was decreased for the AFDD Model01 waveform by about 2%, while it was increased for the four-per-rev and closed loop flap motion by about 1%. However, experimental accuracy for rotor load measurements is also in the 1% to 2% range, so caution is advised in applying these results.

Changes in the vibratory hub loads, derived from hub-based accelerometer measurements, are shown in Figure 15c. The AFDD Model01 waveform tends to introduce the most vibrations in the higher harmonics range (two-per-rev to eight-per-rev), while the four-per-rev active flap motion has the tendency to incur strong vibratory contents mainly in the one-per-rev. Results also indicate that all three "best" active flap motions resulted in the reduction of in-plane (*X*-*Y*) vibrations associated with higher harmonics, but not necessary at one-per-rev. In addition, some penalties in the vibration in the normal (*Z*) direction are evident.

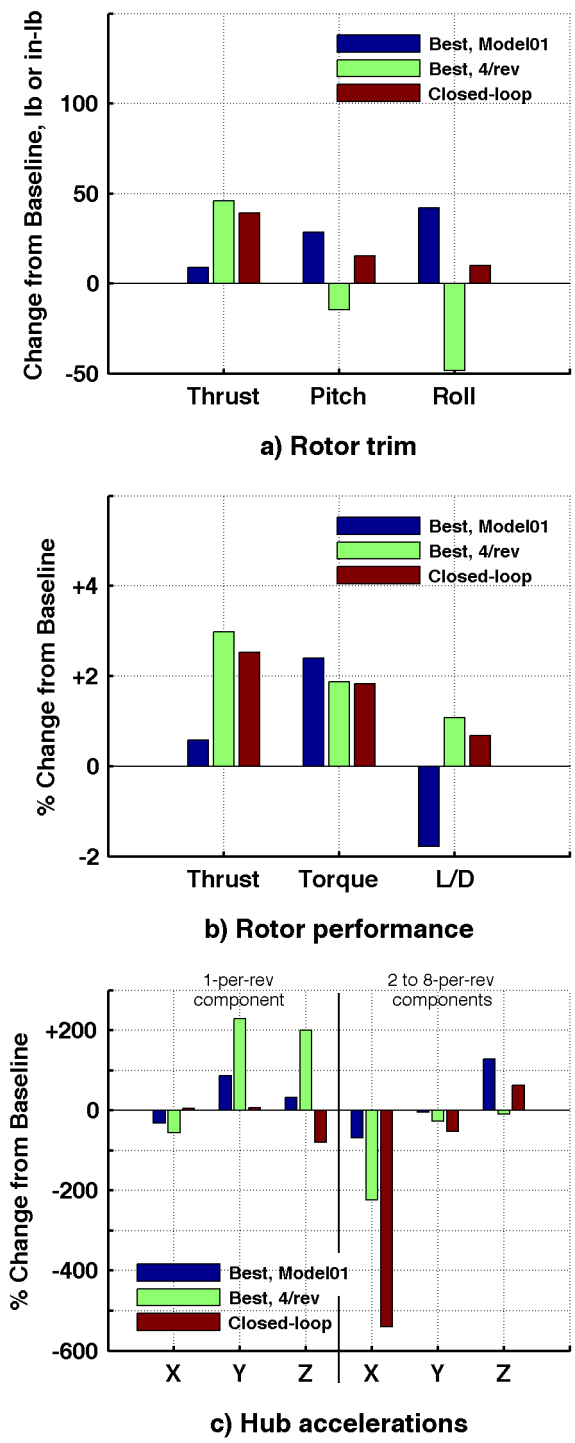

Figure 15. Comparisons of rotor trim, rotor performance and hub vibrations for "best" active motion schemes.

CONCLUSIONS

Results in this paper reported a first-of-its-kind exploration of localized, non-harmonic active flap motions to address low frequency, in-plane rotor noise mitigations. Operational feasibility was demonstrated via testing of the full-scale AATD/Sikorsky/UTRC active flap demonstration rotor in the NFAC's 40- by 80-Foot anechoic wind tunnel. An in-plane microphone array was used to capture the directivity of rotor noise radiation, forward and near in-plane of the rotor in the near-field. Although low frequency noise measurement were compromised by reflections due to non-ideal wind tunnel wall treatment and facility effects, qualitative interpretations of measured noise data demonstrated potential acoustics benefits of the use of localized, non-harmonic active flap motions without significant performance penalties.

For the nominal operating condition at 415 RPM and 120 knots wind tunnel speed studied in this paper, major findings included:

- Use of localized, non-harmonic active flap motions, AFDD Model01 waveform, resulted in low frequency rotor noise reductions over the entire in-plane microphone array.
- Effectiveness of the AFDD Model01 waveform was similar to conventional four-per-rev flap motion. The latter demonstrated similar noise reduction levels over the in-plane microphone array.
- First successful implementation of closed-loop acoustics that resulted in noise reductions over the entire in-plane microphone array.
- Forward, in-plane noise reductions were achieved via deploying the active flap motions in the same manner on the advancing side of the rotor for all three approaches. Subsequently, blade torsion dynamics introduced on the advancing side of the rotor were also similar. This feature is key for generating "anti-loading noise" to cancel noise radiating forward and near the plane of the rotor.
- Torque penalty for the "best" AFDD Model01 waveform was about 2.3% - a value comparable to the "best" four-per-rev case and the closed-loop case. In general, all three approaches led to a minor impact of rotor aerodynamic efficiencies of less than ±2%.
- The "best" AFDD Model01 waveform incurred strongest vibration levels at frequencies two-per-rev and above. At one-per-rev, engaging the active flaps with AFDD Model01 waveform generated only a modest increase in vibrations, compared to almost 220% increase for the four-per-rev flap.

These results suggest that the AFDD Model01 waveform, proposed purely for noise mitigation in this study, is not suitable, as yet, for simultaneous reduced noise, reduced vibrations and improved rotor performance operations. However, such localized, non-harmonic active flap motion has the potential to be refined, perhaps in future tests, to explore supplementary active flap motions at non-advancing side rotor azimuths, to concurrently address performance/vibration concerns.

ACKNOWLEDGMENTS

The rotor fabrication, whirl testing, wind tunnel testing, and data analysis efforts were conducted under TIA W911W6- 08-2-0004 between Sikorsky Aircraft and the U.S. Army AATD. Mr. David Friedmann and Mr. William Harris were the respective AATD and Sikorsky Program Managers. The efforts of the entire Sikorsky/UTRC design, analysis, and test teams and the NFAC/AFDD/NASA test operations, acoustics, and safety review team are gratefully acknowledged. In particular, special thanks to Dr. William Warmbrodt and Mr. Alex Amy (both from NASA Ames); and Mr. Thomas Maier and Dr. Mark Fulton (both from AFDD) for their advice and consultations.

REFERENCES

1. Yu, Y. H., Gmelin, B., Splettstoesser, W., Philippe, J. J. Prieur, J. and Brooks, T. F., "Reduction of Helicopter Blade-Vortex Interaction Noise by Active Rotor Control Technology," *Prog. Aerospace Sci.*, Vol. 33, pp. 647-687, 1997.
2. Jacklin, S. A., Blaas, A., Teves, D., and Kube, R., "Reduction of Helicopter BVI Noise, Vibration and Power Consumption Through Individual Blade Control," American Helicopter Society 51st Annual Forum & Technology Display, May 1995.
3. Marcolini, M. A., Booth, E. R., Tadghighi, H., Hassan, A. A., Smith, C. D. and Becker, L. E., "Control of BVI Noise Using an Active Trailing-Edge Flap," American Helicopter Society San Francisco Bay Area Chapter's Vertical Lift Aircraft Design Conference, San Francisco, CA, January 1995.
4. Booth, E. R. Jr. and Wilbur, M. L., "Acoustic Aspects of Active-Twist Rotor Control," American Helicopter Society 58th Annual Forum &

Technology Display, Montreal, Canada, June 11-13, 2002.

5. Sim, B. W., "Suppressing In-Plane, Low Frequency Helicopter Harmonic Noise with Active Controls," American Helicopter Society San Francisco Bay Area Chapter's Aeromechanics Specialist's Meeting, Fisherman's Wharf, CA, January 2008.
6. Gopalan, G. and Schmitz, F. H.,, "Far-Field Near In-Plane Harmonic Main Rotor Helicopter Impulsive Noise Reduction Possibilities," American Helicopter Society 64th Annual Forum & Technology Display, Montreal, Canada, April 29 – May 1, 2008.
7. Sim, B. W., Janakiram, R. D., Barbely, N. L. and Solis, E., "Reduced In-Plane, Low Frequency Noise of an Active Flap Rotor," American Helicopter Society 65th Annual Forum & Technology Display, Grapevine, TX, May 27-29, 2009.
8. Fogarty, D. E., Wilbur, M. L. & Sekula, M. K., "The Effect of Non-Harmonic Active Twist Actuation on BVI Noise," American Helicopter Society 67th Annual Forum & Technology Display, Virginia Beach, VA, May 3-5, 2011.
9. Sargent, D. C. and Schmitz, F. H., "Fundamental Experimental Studies Supporting On-Blade Tip Air Blowing Control of In-Plane Rotor Harmonic Noise," American Helicopter Society 68th Annual Forum & Technology Display, Fort Worth, TX, May 1-3, 2012.
10. Lorber, P., O'Neil, J., Hein, B., Isabella, B., Andrews, J., Brigley, M., Wong, J., LeMasurier, P. and Wake, B., "Whirl and Wind Tunnel Testing of the Sikorsky Active Flap Demonstration Rotor," American Helicopter Society 67th Annual Forum & Technology Display, Virginia Beach, VA, May 3-5, 2011.
11. Lorber, P., Hein, B., Wong, J. and Wake, B., "Rotor Aeromechanics Results from the Sikorsky Active Flap Demonstration Rotor," American Helicopter Society 68th Annual Forum & Technology Display, Fort Worth, TX, May 1-3, 2012.
12. Chaudhry, Z. A., Wake, B. E., Bagai, A., Lorber, P. F. and Collons, A. J., "Active Rotor Development for Primary and Secondary Flight Control," American Helicopter Society 65th Annual Forum & Technology Display, Grapevine, TX, May 27-29, 2009.
13. Andrews, J., Wong, J. and Brigley, M., "Dynamics of a High-Authority Active Flap Rotor," American Helicopter Society 68th Annual Forum & Technology Display, Fort Worth, TX, May 1-3, 2012.
14. Barbely, N. L., Sim, B. W., Kitaplioglu, C. K. and Goulding II, P., "Acoustics Reflection of Full-Scale Rotor Noise Measurements in NFAC 40- by 80-Foot Wind Tunnels," American Helicopter Society Aero-mechanics Specialists' Conference, San Francisco, CA, January 20-22, 2010.